Some Regularities of Ion Sheath Dynamics at High Voltage Pulses[1]

E.V. Nefyodtsev and G.E. Ozur

Institute of High-Current Electronics SB RAS, 2/3, Akademicheskii ave., Tomsk, 634055, Russia
E-mail: nev@lve.hcei.tsc.ru

Abstract – The time evolution of an unsteady ion sheath in the presence of cylindrical protrusions at the cathode is studied numerically in a two-dimensional model. The calculations demonstrate the enhancement of the electric field and the focusing of the ion flow at the protrusion vertices. It is shown that, in the stage of the sheath formation, in addition to the electrostatic focusing of the ion flux, there is also focusing caused by the curvature of the plasma boundary around a protrusion. The results of calculations agree satisfactorily with the experimental data on the delay time of explosive emission at the multi-wire cathode of a high-current plasma-filled diode. For the case of planar cathode, the analytical formulas for maximum values of electric field strength and ion current density are obtained.

1. Introduction

Studies of the dynamics of the cathode ion sheath are important for understanding the processes occurring in high-current plasma-filled electron guns with explosive-emission cathodes, plasma immersion ion implantation devices and other electro-physical devices, including vacuum circuit breakers and switches [1–3].

Calculations made in [4, 5] for the planar cathode, have shown the significant peaks of electric field strength, E_C, and ion current density, J_C, at the cathode which are caused by the fast rising of the voltage during sheath formation. Actually, if the voltage rise time τ is compared or lower than ion transit time across the sheath, so the thickness of the latter is essentially lower than the thickness of Child–Langmuir sheath (CLS). This leads to the above-mentioned peaks of E_C and J_C, which then gradually decreases to the steady-state values.

Since the time delay of micro-points explosion depends strongly on electric field strength, so the emitting elements with small-radius-curvature vertices (such as ring protrusions, fine wires, blades, teeth, or graphite filament bunches) are placed at certain intervals on the cathode substrate [6]. For vacuum diodes, there are calculated data [7] on the field strength for different emitter geometries. For plasma-filled diodes, the corresponding calculation technique is still lacking.

Along with micro-points explosion, the breakdown of non-metallic inclusions and films on the cathode under their charging with ion current from plasma plays an important role in emission centers initiation. Correct measurements of ion current density with spatial resolution of about the characteristic diameter of the emitter (~ 100 μm) are practically impossible. That is why the calculations of J_C are actual from this point of view as well.

In this study, we performed 2D calculations of the electric field strength and ion current density in the non-steady ion sheath near a cathode with emitters in the shape of cylindrical protrusions on a plane substrate. Plasma parameters and protrusion size were chosen in correspondence with experiment [8] where the excitation of explosive emission at the multi-wire cathode was investigated.

2. Model

It is assumed that no emission from the cathode. Plasma with density up to 10^{19} m^{-3} is proposed to be collisionless. Plasma electrons energy distribution corresponds to Boltzmann's distribution. In the case of cylindrical symmetry, the set of equations describing the plasma and the electric field is well known:

$$\frac{\partial(rN)}{\partial t}+\frac{\partial(rNv_r)}{\partial r}+\frac{\partial(rNv_z)}{\partial z}=0\,, \qquad (1)$$

$$\frac{\partial v_r}{\partial t}+v_r\frac{\partial v_r}{\partial r}+v_z\frac{\partial v_r}{\partial z}=-\frac{q_0}{M}\frac{\partial \varphi}{\partial r}\,, \qquad (2)$$

$$\frac{\partial v_z}{\partial t}+v_r\frac{\partial v_z}{\partial r}+v_z\frac{\partial v_z}{\partial z}=-\frac{q_0}{M}\frac{\partial \varphi}{\partial z}\,, \qquad (3)$$

$$\frac{\partial}{\partial r}\left(r\frac{\partial \varphi}{\partial r}\right)+\frac{\partial}{\partial z}\left(r\frac{\partial \varphi}{\partial z}\right)=-\frac{q_0}{\varepsilon_0}r\left[N-N_0\exp\left(\frac{q_0\varphi}{kT_e}\right)\right]. \qquad (4)$$

where r and z are the radial and axial coordinates, respectively; N is the ion density; φ is the electrostatic potential; V_r and V_z are the radial and axial components of the ion drift velocity, respectively; q_0 is the elementary charge; M is the ion mass; k is the Boltzmann constant; and T_e is the electron temperature.

Equation (1) is the continuity equation for ions. Equations (2) and (3) describe the radial and axial components of ion velocity, respectively. Poisson's

[1] The work was supported by the Russian Foundation for Basic Research (Project No. 06-02-96905) and Russian Federal Agency on Science and Innovations (Contract No. 02.516.11.6094).

equation (4) describes the electrostatic potential distribution.

The set of equations was solved with the following boundary and initial conditions.

The cathode potential increases linearly during time τ, and remains constant after that:

$$\varphi(z_C, r_C t) = -U(t) = \begin{cases} -U_0 t/\tau, & t \le \tau; \\ -U_0, & t > \tau. \end{cases}$$

Inside plasma volume parameters are as follows: $\varphi = 0$; $N = N_0$; $V_z = V_r = 0$.

At the axis ($r = 0$) and at distant (imaginary) wall ($r = R$), all the radial derivatives are zero.

It was assumed that, at the initial instant $t = 0$, plasma is uniform $N(z, r, 0) = N_0$. The ion drift velocity and the potential at $t = 0$ were assumed to be zero.

3. Results and discussion

A. Electric field and ion flux peaks

Consider the results obtained for plasma parameters from the experiments [8]: $N_0(\mathrm{Ar}^+) = 5 \times 10^{18}$ m^{-3}, $\tau = 70$ ns, and $U_0 = 20$ kV. Cylindrical protrusion of diameter $d_P = 0.1$ mm and height $h_P = 1$ mm has a semispherical peak.

Figure 1 shows the time dependences of the absolute values $E_C(t)$ and $J_C(t)$ at the peak of protrusion (P) and far from, i.e., on the planar part of the cathode. Dashed line shows the steady-state values of the field and ion current density, E_{St}, J_{St}, established after time interval $t > 10$ μs.

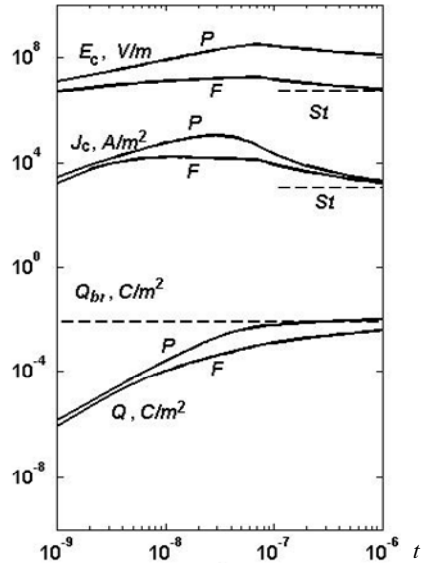

Fig. 1. Time dependences of the field strength and ion current density at the cathode as well as ion charge density. Index P signifies peak of protrusion and F (flat) – planar part of the cathode

Note the following peculiarities of the dependences $E_C(t)$ and $J_C(t)$.

1) Electric field strength achieves its maximum $E_C^{\max}$ at $t = \tau$ at any point of the cathode surface. Ion current density achieves its maximum $J_C^{\max}$ at $t < \tau$, at that, in different times for different points of the cathode. The decrease of $J_{C\text{-}F}$ starts already at voltage rise time at $t \sim 2(\omega_i)^{-1}$, where ω_i is the ion-plasma frequency. At $t = \tau$ the decreasing rate is noticeably increases. At the protrusion peak, the decrease of $J_{C\text{-}P}$ starts later and at $t = \tau$ the decreasing rate changes weakly.

2) The $E_{C\text{-}F}$ and $E_{C\text{-}P}$ values distinguish essentially in any time moment. The most distinguishing is achieved at $t = \tau$. For this case the ratio is

$$(E_{St}):(E_{C\text{-}F}^{\max}):(E_{C\text{-}P}^{\max}) = (1):(3.5):(59).$$

For the ion current density this ratio is

$$(J_{St}):(J_{C\text{-}F}^{\max}):(J_{C\text{-}P}^{\max}) = (1):(15.6):(105).$$

The $J_{C\text{-}F}$ and $J_{C\text{-}P}$ values are distinguish essentially during the limited time only.

For the planar part of the cathode, calculations allowed us to obtain the following analytical formulas:

$$E_{C-F}^{\max} = 1.72 \cdot 10^{-4} \mu^{0.1625} Z^{0.175} N_0^{0.3375} U_0^{0.5} \tau^{-0.325} \text{ [V/m]};$$

$$J_{C-F}^{\max} = 7.58 \cdot 10^{-16} \mu^{-0.25} N_0^{0.75} U_0^{0.5} \tau^{-0.5} \text{ [A/m}^2\text{]},$$

where μ is the ion mass (aum); Z is the ion charge (in units of elementary charge); N_0 is the plasma density (m^{-3}); τ is the voltage rise time duration (s); U_0 is the voltage pulse amplitude (V).

The time moment of current maximum may be estimated according to formula

$$t_{J\max} = 4.64 \mu^{0.425} Z^{-0.85} N_0^{-0.425} T^{0.15} U_0^{-0.15} \tau^{0.15} \text{ [s]},$$

where T is the temperature of electrons (eV).

B. Focusing effects

Basing on calculations, it has been established that the main reason of the strong difference between $J_{C\text{-}P}(t)$ and $J_{C\text{-}F}(t)$ is the focusing caused by the curvature of plasma emission boundary not electrostatic focusing.

Figure 2 shows the combined image of potential and ion density distribution at different times. At the initial stage ($t < 3$ ns), when plasma boundary is closer to the protrusion surface, the ion motion runs like in planar sheath (Fig. 2, *a*). As far as the distance between plasma boundary and protrusion becomes to be comparable with the radius of latter, so the ion motion may be considered as in semispherical gap providing parabolic growth of ion density toward the protrusion peak (Fig. 2, *b*). As is evident, ion density changes non-monotonically. At $t = 100$ ns, plasma boundary moves away so much that becomes practically parallel to the cathode plate and "geometrical" focusing disappears (Fig. 2, *c*). Thus, calculations show that electrostatic focusing is ineffective in our case.

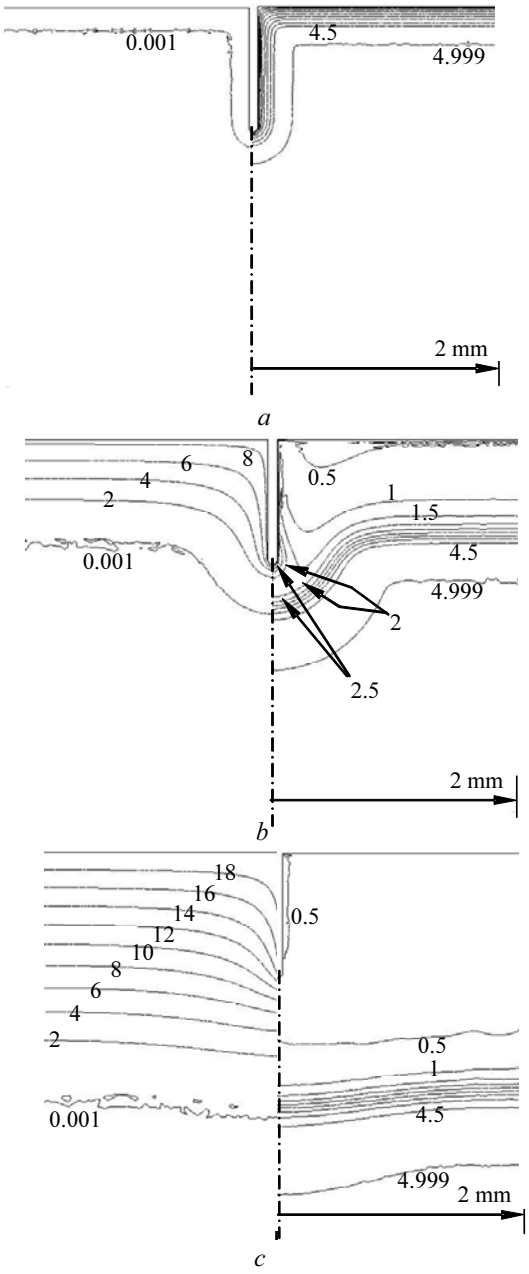

Fig. 2. The combined image of potential (at the left) and ion density distribution (at the right) at different times: *a* – 3 ns; *b* – 30 ns; *c* – 100 ns. Potential values at equipotential curves are given in kV [0.001; 2; 3; …, 20]. Values of ion density are given in units 10^{18} m^{-3} [0.5; 1.0; 1.5; …4.5; 4.999]. $N_0 = 5 \times 10^{18}$ m^{-3}; $\tau = 70$ ns

C. Influence of the surrounding protrusions

From the practical point of view, the calculations of E_C and J_C at the peak of protrusion surrounded with analogues protrusions is of most importance. In 2D approximation, the influence of surrounding protrusions was modelled by rings.

R-Z-cross section of the rings was assumed as for central protrusion. The effect of several rings having radii $r = \Delta R; 2\Delta R\ldots$ was investigated. Calculations were performed for typical values $\Delta R = 0.5$–2 mm. Results of calculations are presented in Fig. 3.

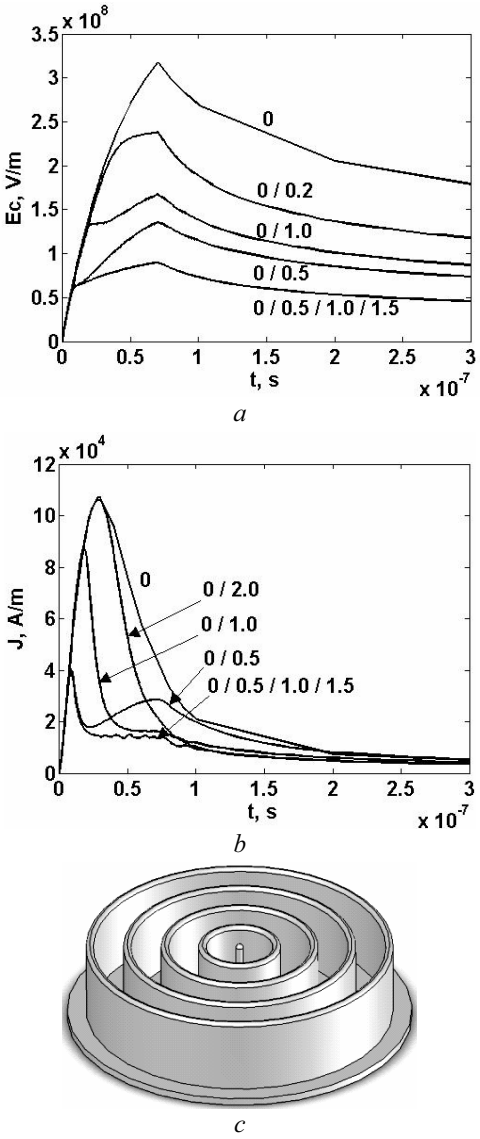

Fig. 3. Time dependences of the field strength (*a*) and ion current density (*b*) at the peak of protrusion surrounded with rings. Numbers means radial coordinates of the corresponding rings taking into account under calculations (0 – single protrusion). Image of the cathode (*c*)

The most influence on dependences $E_C(t)$ and $J_C(t)$ is given by the ring nearest to the central protrusion. The influence decreases with the increase of the ring radius. At the initial stage time, dependences $E_C(t)$ and $J_C(t)$ correspond to those obtained for a single protrusion. When the cathode sheath thickness becomes comparable with ΔR, the essential deviations of $E_C(t)$ and $J_C(t)$ curves from those obtained for a single protrusion are observed.

Electrostatic screening given by rings always leads to decreasing $E_{C\text{-}P}^{\max}$ value (Fig. 3, *a*). However, changing of $J_{C\text{-}P}^{\max}$ begins at $\Delta R < 2$ mm (Fig. 3, *b*). At lower ΔR values, the non-monotone behavior of

$J_{C\text{-}P}(t)$ dependences becomes apparent, but is smoothed as higher amount of surrounding rings are taken into account (Fig. 3, *b*). The second maximum on $J_{C\text{-}P}(t)$ curves is achieved at $t = \tau$.

As evident, as ΔR decreases and number of surrounding rings increases, the dependences $E_{C\text{-}P}(t)$ and $J_{C\text{-}P}(t)$ approach to $E_{C\text{-}F}(t)$ and $J_{C\text{-}F}(t)$ dependences, respectively.

Replacing the solid rings by discrete protrusions should provide some growth of the electric field strength and ion current density.

D. Estimations of the significance of the factors responsible to emission centers appearance

Results obtained in [8] testify to appearance of the explosive-emission centers within 20–30 ns after the voltage pulse start. The present calculations have shown that $E_{C\text{-}P}^{\max}$ does not achieve tens of MV/cm needed for intensive field emission. Thus, explosive emission is possible if sub-micro-points with enhancement coefficient of several tens are presented on the peaks of protrusions.

The other way of emission centers initiation is concluded in breakdown of local dielectric inclusion on the cathode. The breakdown condition is as follows [9]:

$$Q(t) = \int_0^t J_C(t')dt' \geq Q_{br} = \varepsilon_0 \varepsilon E_{br}, \qquad (5)$$

where $\varepsilon_0\varepsilon$ is the absolute dielectric permittivity and E_{br} is the electric strength of the inclusion (film) material. Fig. 1 also gives the dependences $Q(t)$ obtained by integrating of $J_C(t)$. Dashed line indicates Q_{br} for typical values $\varepsilon = 3$ and $E_{br} = 3 \cdot 10^8$ V/m. It is evident, that ion current density on the peaks of protrusions is quite enough to cause the inclusion breakdown within tens of nanoseconds. Thus, this mechanism plays very important role in initiation of emission centers (cathode spots).

4. Conclusions

1. A method has been developed for two-dimensional numerical simulations of the highly non-uniform electric field and ion current density in an unsteady cathode sheath. The time evolution of the electric field strength and ion current density has bean calculated near a cylindrical protrusion on the cathode surface.

2. It is shown that, within a finite time interval during the voltage rise, the ion flow is additionally focused due to the curvature of the plasma boundary around the protrusion.

3. The results of calculations of the density of the focused ion flow agree satisfactorily with the experimental data on the delay time of explosive emission at the multi-wire cathode of a high-current plasma-filled diode.

Acknowledgements

We are grateful to Prof. D.I. Proskurovsky and to Prof. A.V. Kozyrev for their continuous interest in this study and helpful discussions.

References

[1] G.E. Ozur, D.I. Proskurovsky, V.P. Rotshtein, and A.B. Markov, Laser & Particle Beams **21**, No. 2, 157 (2003).

[2] G.A. Collins and J. Tendys, Plasma Sources Sci. Technology **3**, 10 (1994).

[3] P. Sarrailh, L. Carrigues, G.J.M. Hagelaar et al., J. Phys. D: Appl. Phys. **41**, 015203 (11 pp) (2008).

[4] R.A. Stewart and M.A. Lieberman J. Appl. Phys. **70** (7), 3481 (1991.).

[5] M.Yu. Kreindel, E.A. Litvinov, G.E. Ozur, and D.I. Proskurovsky, Fiz. Plazmy **17**, 1425 (1991).

[6] G.A. Mesyats and D.I. Proskurovsky, *Pulsed Electrical Discharge in Vacuum*, Berlin, Springer-Verlag, 1989.

[7] I.N. Slivkov, *Electrical Insulation and Discharge in Vacuum*, Moscow, Atomizdat, 1972.

[8] G.E. Ozur, D.I. Proskurovsky, and K.V. Karlik, Izv. Vyssh. Uchebn. Zaved. Fiz., No. 11 22 (2006).

[9] Lutz M.A., IEEE Trans. Plasma Sci. **2**/ 1, 1 (1974).